Original Article

Quantitative assessment of early changes in myocardial extracellular volume during postoperative adjuvant chemotherapy in patients with breast cancer via dual-layer spectral detector computed tomography: a cohort study

Honglin Wu[1,2#], Yan Huang[1,2#], Meng Yang[1], Zhiheng Lu[1], Weiwei Deng[3], Yu Wang[3], Qin Xiao[1,2*], Yajia Gu[1,2*]

[1]Department of Radiology, Fudan University Shanghai Cancer Center, Shanghai, China; [2]Department of Oncology, Shanghai Medical College, Fudan University, Shanghai, China; [3]Clinical & Technical Support Department, Philips Healthcare, Shanghai, China

Contributions: (I) Conception and design: H Wu, Y Huang, W Deng, Q Xiao, Y Gu; (II) Administrative support: Q Xiao, Y Gu; (III) Provision of study materials or patients: M Yang, Z Lu, H Wu; (IV) Collection and assembly of data: H Wu, Y Huang; (V) Data analysis and interpretation: H Wu, Y Wang, Q Xiao; (VI) Manuscript writing: All authors; (VII) Final approval of manuscript: All authors.

[#]These authors contributed equally to this work as co-first authors.

[*]These authors contributed equally to this work.

Correspondence to: Yajia Gu, PhD; Qin Xiao, MD. Department of Radiology, Fudan University Shanghai Cancer Center, 270 East Shore Road, Shanghai 200072, China; Department of Oncology, Shanghai Medical College, Fudan University, Shanghai, China. Email: guyajia@126.com; xrayctmrixiao@163.com.

Background: The major of anticancer therapies induce a wide spectrum of cardiotoxic effects. Early identification of anticancer treatment-associated cardiotoxicity is critical to informing decisions on subsequent interventions. Myocardial extracellular volume (ECV) has been proposed as a useful parameter for quantifying the early cardiotoxicity of cancer-related treatment. This study used dual-layer spectral detector computed tomography (CT) technology to simultaneously assess cardiac function and myocardial ECV, characterizing the early changes in parameters during breast cancer therapy.

Methods: A single-center cohort study was conducted that prospectively enrolled 40 women with breast cancer (mean age 47.5±10.8 years) who underwent postoperative adjuvant chemotherapy between January 12, 2022, and November 2, 2023, with available data from baseline to 3 months after chemotherapy of cardiac computed tomography (CCT), ultrasound cardiography (UCG), electrocardiography, and serum biomarkers. Midventricular and global ECVs of the left ventricle were measured based on an iodine map of the late enhancement phase of dual-layer spectral detector CT. Changes in cardiac function parameters, ECVs, and cardiac biomarkers from baseline to the 3-month follow-up were analyzed. Correlation coefficients between the changes in cardiac function parameters and ECVs were calculated.

Results: Between baseline and 3 months, there was no significant change in left ventricular ejection fraction (LVEF) on UCG (67.1%±3.8% *vs.* 66.3%±4.3%, P=0.29) or LVEF on CCT (65.4%±5.9% *vs.* 64.3%±7.4%, P=0.28). Heart rate increased over 3 months of follow-up (75.2±11.5 *vs.* 81.7±12.3 bpm; P<0.01). After normalization to body surface area (BSA), cardiac output on CCT/BSA ratio (CCT-CO indexed) [3.5±0.6 *vs.* 3.8±0.6 L/(min·m^2); P=0.01] and left ventricular late (active) filling volume/BSA ratio (LVLFV indexed) (13.5±3.7 *vs.* 15.8±4.2 mL/m^2; P<0.01) significantly increased, while there was a significant decrease at the 3-month follow-up in left ventricular early (passive) filling volume/BSA ratio (LVEFV indexed) (33.3±6.6 *vs.* 30.6±8.2 mL/m^2; P=0.01) and LVEFV/LVLFV ratio (2.7±1.1 *vs.* 2.1±0.9; P<0.01). Midventricular and global

ECVs were elevated at 3 months, significantly so for the midanterior ECV (24.0%±4.5% *vs.* 25.6%±3.1%; P=0.04), midaverage ECV (25.6%±2.5% *vs.* 27.0%±2.9%; P=0.01) and global ECV (25.4%±2.4% *vs.* 27.3%±2.7%; P<0.01). Although changes in ECVs were not associated with changes in LVEFs, global ECV changes were moderately correlated with changes in left ventricular end-diastolic volume/BSA ratio (CCT-LVEDV indexed) (r=0.52; P<0.001), left ventricular stroke volume/BSA ratio (CCT-LVSV indexed) (r=0.56; P<0.001), CCT-CO indexed (r=0.40; P=0.01), and LVEFV indexed (r=0.41; P=0.009).

Conclusions: CCT-derived ECV was used to evaluate myocardial changes in the early stage of chemotherapy before LVEF significantly decreased. The increases in ECV were not correlated with LVEF. The changes in myocardial ECVs were moderately correlated with cardiac function parameters. ECV may be a useful biomarker for detecting cardiotoxicity in patients with breast cancer in the early stage of anticancer therapy.

Keywords: Breast cancer; cardiac computed tomography (CCT); myocardium; extracellular volume; cardiotoxicity

Submitted Apr 16, 2024. Accepted for publication Nov 01, 2024. Published online Dec 30, 2024.
doi: 10.21037/qims-24-777
View this article at: https://dx.doi.org/10.21037/qims-24-777

Introduction

With the diversification of anticancer treatment regimens, the survival time of patients with breast cancer has been extended, and the survival rate has increased. Cancer therapy-related cardiac dysfunction caused by anticancer treatments has become a common cause of death among cancer survivors (1-4), severely impacting patient prognosis and quality of life. Therefore, the early detection and monitoring of the cardiotoxicity induced by anticancer agents are essential.

Research suggests that chemotherapy-induced cardiotoxicity is a process that begins with subclinical myocardial damage, leads to an asymptomatic decline in left ventricular ejection fraction (LVEF), and finally progresses to symptomatic heart failure (5). As the most commonly used diagnostic and monitoring indicator, LVEF measured by ultrasound cardiography (UCG) has poor repeatability and is not sufficiently sensitive for the monitoring of subclinical myocardial injury (6,7). Myocardial extracellular volume (ECV) may have the potential to quantify chemotherapy-induced cardiotoxicity, in which acute myocardial edema or subsequent fibrosis due to cardiotoxicity can increase the ECV (8,9). ECV measured by cardiac magnetic resonance (CMR) has recently been developed for quantifying cardiotoxicity caused by anticancer drugs, as recommended in many guidelines (10,11). Computed tomography (CT)-derived ECV correlates well with CMR-derived ECV and histology (12-14). Compared with CMR, cardiac computed tomography (CCT) by dual-layer spectral detector CT, as a new technology for quantifying ECV, can simultaneously evaluate cardiac function and myocardial ECV; this technique is faster, easier to implement, and has particular advantages for patients with contraindications to magnetic resonance imaging (MRI) (15).

Only a few studies have been conducted on CT-derived ECVs for detecting cardiotoxicity, most of which used chest enhanced scanning (16-19) and lacked electrocardiogram-gated scanning, resulting in possible motion artifacts and high intraindividual variability. Only Egashira *et al.* (20) used cardiac CT scanning to analyze late-phase cardiotoxicity in patients with breast cancer. The cardiotoxicity assessed by CT-derived ECV in the early phase after chemotherapy remains to be defined, and are no reports on CT-derived ECV myocardial segmental analysis or on the correlation between ECV measured by CT and cardiac function parameters.

Anthracycline-based chemotherapy is the mainstay of breast cancer treatment, but it involves dose-dependent cardiotoxic side effects. Therefore, our primary objectives in this study were to quantify the changes in myocardial ECV on CCT and cardiac function parameters by CCT and UCG in the early stage of chemotherapy (with epirubicin) in patients with breast cancer. We further analyzed the correlations between the changes in cardiac function parameters and the changes in ECV. We present this article in accordance with the STROBE reporting checklist (available at https://qims.amegroups.com/article/view/10.21037/qims-24-777/rc).

Methods

Study participants

Adult women with stage I to III breast cancer who were scheduled to undergo postoperative adjuvant epirubicin-containing chemotherapy (Table S1) were prospectively recruited from January 12, 2022, to November 2, 2023 from Fudan University Shanghai Cancer Center. CCT, two-dimensional (2DE) UCG performed on a Vivid E90 device (GE HealthCare, Chicago, IL, USA), serum biomarker measurements, and electrocardiography were performed both before and 3 months after treatment. The exclusion criteria were as follows: (I) general contraindications to the administration of iodinated contrast agents; (II) a life expectancy of less than 24 months; (III) prior exposure to chemotherapy or radiotherapy; (IV) current or prior congenital heart disease, myocardial infarction, or heart failure; (V) absence of 3-month follow-up or incomplete data (lacking data for UCG, serum biomarkers, or CCT at baseline or at 3 months); (VI) a change in antitumor treatment plans or discontinued treatment; and (VII) poor image quality. To reduce selection bias, clinicians screened patients strictly according to preset inclusion and exclusion criteria to ensure sample consistency; in addition, the purpose of the study was explained in full to patients through popular science videos to improve the participation rate and understanding of patients. To reduce observer bias, all examinations and parameter measurements were double-blinded. In order to reduce loss of access bias, patients were regularly followed up by dedicated staff.

This study was conducted in accordance with the Declaration of Helsinki (as revised in 2013) and was approved by the Ethics Committee of Fudan University Shanghai Cancer Center (No. 2111245-25; approved on November 30th, 2021). Written informed consent was obtained from all participants in the study.

CCT acquisition protocols

All images were acquired with the patient in the supine position with a dual-layer spectral detector CT (IQon; Philips Healthcare, Best, the Netherlands). The contrast agent used was iodinated (320 mg/mL iodine; Jiangsu Hengrui Pharmaceuticals Co., Ltd., Lianyungang, China). The CCT protocol involved a coronary CT angiography (CCTA) scan and a delayed phase of 7 minutes after injection. Details of the CCT acquisition are summarized in Appendix 1.

CCT data analysis

All images were reconstructed via a dedicated workstation (IntelliSpace Portal 10.0, Philips Healthcare). In the CCTA images, cardiac parameters were automatically analyzed by the workstation. The spectral-based image data of the delayed phase were postprocessed to generate a myocardial ECV map (14), and the average ECV was calculated (*Figure 1A*,*1B*) (21). The global ECV was derived from an average of 17 myocardial segments (22,23). To obtain the iodine value of the myocardium, six regions of interest (ROIs) were drawn in the middle of the left ventricular short axis at the systolic phase. To obtain the iodine value of the blood pool, a ROI was placed in the left ventricular cavity at the same level as the myocardial ROIs. The ECV map was calculated with the following formula (12,24):

$$ECV = (1 - HCT) \times \frac{Iodine\ concentration\ in\ the\ myocardium}{Iodine\ concentration\ in\ the\ blood} \quad [1]$$

where HCT is the hematocrit level. The iodine concentration was measured on iodine images in milligrams per milliliter (mg/mL).

All ventricular volumes and masses were normalized to body surface area (BSA) as calculated using the Mosteller formula (25).

Definition of cancer therapy-related cardiac dysfunction

Symptomatic or asymptomatic cancer therapy-related cardiac dysfunction was defined based on the 2022 European Society of Cardiology (ESC) guidelines (26).

Statistical analysis

Statistical analysis was performed with SPSS 26 (IBM Corporation, Armonk, NY, USA) software. The Shapiro-Wilk test was used to evaluate the normality of the data. Variables with a normal distribution are expressed as the mean ± standard deviation (SD), whereas nonnormally distributed variables are expressed as the median and 25th and 75th percentiles. Categorical variables are expressed as numbers and percentages. The paired *t*-test or Wilcoxon signed-rank test was used to compare the differences in variables (baseline *vs.* 3 months). Significant differences were assessed via analysis of variance followed by the Fisher

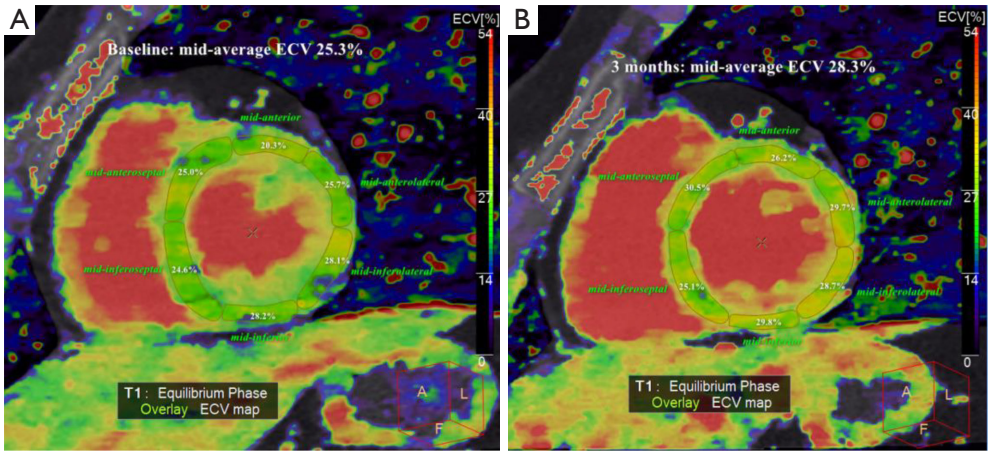

Figure 1 ROI placement in a 28-year-old female patient. (A) ECV map at baseline. (B) ECV map at the 3-month follow-up. In the middle part of the left ventricular short axis, six ROIs were drawn on the ECV map, including the midinferoseptal, midanteroseptal, midanterior, midanterolateral, midinferolateral, and midinferior regions. The midaverage ECV increased from baseline to 3 months (25.3% *vs.* 28.3%). ROI, region of interest; ECV, extracellular volume.

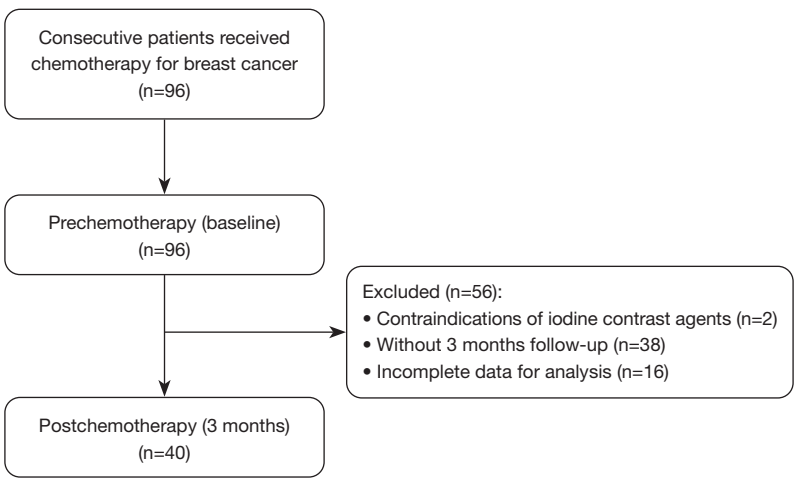

Figure 2 Flowchart of patient inclusion. Ninety-six patients with breast cancer were recruited, and 40 patients remained after the application of the exclusion criteria.

least significant difference test for multiple comparisons. Bivariate correlation was assessed with Pearson method or Spearman method. A P value less than 0.05 was considered to indicate a significant difference.

Based on a previous literature (16), we estimated that a minimum of 25 patients was required to ensure the robustness of our statistical analysis, with an 80% power and 5% significance.

Results

Study participants

Initially, 96 patients were included, among whom 56 were excluded due to contraindications to iodinated contrast agents (n=2), lack of follow-up (n=38), or incomplete data for analysis (n=16). Therefore, 40 patients remained for enrollment in this study (*Figure 2*). The baseline

Table 1 Baseline characteristics of the study population

Characteristic	Values (N=40)
Age, mean (SD), years	47.5 (10.8)
Sex (female), n (%)	40 (100.0)
Height, mean (SD), cm	159.7 (3.7)
Weight, mean (SD), kg	60.4 (8.2)
Waist, mean (SD), cm	81.9 (8.5)
Systolic pressure, mean (SD), mmHg	122.6 (18.4)
Diastolic pressure, mean (SD), mmHg	76.3 (10.3)
Cardiovascular disease, n (%)	3 (7.5)
Diabetes, n (%)	2 (5.0)
Hypertension, n (%)	6 (15)
Dyslipidemia, n (%)	23 (57.5)
Chronic kidney disease, n (%)	0
Smoking, n (%)	0
HFA-ICOS risk, n (%)	
Low risk	36 (90.0)
Moderate risk	4 (10.0)
High risk	0
Very high risk	0
Baseline medications, n (%)	
ACE inhibitor	1 (2.5)
Angiotensin receptor blocker	1 (2.5)
β-blocker	1 (2.5)
Calcium channel blocker	3 (7.5)
Statin	1 (2.5)
Any cardiac medication	1 (2.5)
Histologic type (invasive carcinoma), n (%)	40 (100.0)
Breast cancer stage, n (%)	
I	12 (30.0)
II	27 (67.5)
III	1 (2.5)
Breast cancer side, n (%)	
Left	24 (60.0)
Right	16 (40.0)
Bilateral	0

SD, standard deviation; HFA-ICOS, Heart Failure Association-International Cardio-Oncology Society baseline cardiovascular toxicity risk (left ventricular ejection fraction on echocardiography); ACE, angiotensin-converting enzyme inhibitor.

characteristics and cancer treatment details of the 40 patients (age 47.5±10.8 years) who completed the study are summarized in *Table 1*. The median time of CCT between baseline and the 3-month follow-up was 98 (range, 72–134) days.

Changes in UCG and electrocardiography parameters

LVEF on UCG (UCG-LVEF) and left ventricular fractional shortening on UCG (UCG-LVFS) did not significantly change between baseline and the 3-month follow-up. After normalization to BSA, the parameters measured by UCG, including left ventricular end-systolic volume/BSA ratio (UCG-LVESV indexed), left ventricular end-diastolic volume/BSA ratio (UCG-LVEDV indexed), left ventricular stroke volume/BSA ratio (UCG-LVSV indexed), and cardiac output/BSA ratio (UCG-CO indexed), showed no significant changes. Among the diastolic function parameters, only the mean mitral annular peak early diastolic velocity (e') significantly decreased (P=0.01). Early peak diastolic mitral inflow velocity (E), late peak diastolic mitral inflow velocity (A), the E/A ratio, mean mitral annular peak late diastolic velocity (a'), the e'/a' ratio, and the E/e' ratio did not significantly change between baseline and 3 months (*Table 2*). According to electrocardiography, new sinus tachycardia occurred in four patients and one patient developed a new grade I atrioventricular block at the 3-month follow-up.

Changes in cardiac function parameters on CCT

There were no significant changes in LVEF CCT (CCT-LVEF). Heart rate increased over the 3 months of follow-up (P<0.01). When normalized to BSA, CO on CCT/BSA ratio (CCT-CO indexed) (P=0.01) and left ventricular late (active) filling volume/BSA ratio (LVLFV indexed) (P<0.01) were significantly increased at the 3-month follow-up, while left ventricular early (passive) filling volume/BSA ratio (LVEFV indexed) (P=0.01) and the ratio of LVEFV to LVLFV (LVEFV/LVLFV) (P<0.01) significantly decreased on CCT. LVESV/BSA ratio (CCT-LVESV indexed), LVEDV/BSA ratio (CCT-LVEDV indexed), LVSV/BSA ratio (CCT-LVSV indexed), left ventricular mass index (LVMI), left ventricular regurgitation volume/BSA ratio (LVRV indexed), and left ventricular regurgitation fraction index (LVRFI) on CCT did not change between baseline and the 3-month follow-up (*Table 3*).

Table 2 UCG parameters in the patients at baseline and at 3-month follow up

Parameter	Baseline	3 months	P value
BSA, m^2	1.6 (1.6, 1.7)	1.6 (1.6, 1.7)	0.17
UCG-LVESV indexed, mL/m^2	17.8±3.8	18.5±4.6	0.24
UCG-LVEDV indexed, mL/m^2	53.8 (46.3, 61.4)	52.9 (48.2, 58.2)	0.44
UCG-LVSV indexed, mL/m^2	36.8 (30.7, 39.4)	35.6 (31.2, 39.8)	0.78
UCG-CO indexed, $L/(min·m^2)$	3.0 (2.6, 3.2)	3.0 (2.8, 3.3)	0.18
UCG-LVEF, %	67.1±3.8	66.3±4.3	0.29
UCG-LVFS, %	37.2±2.9	36.4±3.2	0.20
E, cm/s	71.5 (63.5, 86.8)	67.5 (55.5, 80.0)	0.07
A, cm/s	78.0±16.7	78.0±16.2	>0.99
E/A	0.9 (0.7, 1.3)	0.8 (0.7, 1.2)	0.20
e', cm/s	9.5 (7.0, 12.0)	8.0 (6.3, 10.0)	0.01
a', cm/s	10.8±2.3	10.6±2.5	0.53
e'/a'	0.9±0.4	0.9±0.5	0.49
E/e'	8.5±2.4	8.9±2.9	0.36

Data are presented as mean ± standard deviation or median (Q1, Q3). BSA, body surface area; UCG, ultrasound cardiography; LVESV, left ventricular end-systolic volume; LVEDV, left ventricular end-diastolic volume; LVSV, left ventricular stroke volume; CO, cardiac output; LVEF, left ventricular ejection fraction; LVFS, left ventricular fractional shortening; E, early peak diastolic mitral inflow velocity; A, late peak diastolic mitral inflow velocity; e', mean mitral annular peak early diastolic velocity; a', mean mitral annular peak late diastolic velocity.

Changes in ECV on CCT

As detailed in *Table 4*, the midventricular and global ECVs were elevated. From baseline to 3-month follow-up, these increases were significant for the midanterior ECV (24.0%±4.5% *vs.* 25.6%±3.1%; P=0.04), midaverage ECV (25.6%±2.5% *vs.* 27.0%±2.9%; P=0.01), and global ECV (25.4%±2.4% *vs.* 27.3%±2.7%; P<0.01). The midinferoseptal ECV, midanteroseptal ECV, midanterolateral ECV, midinferolateral ECV, and midinferior ECV were increased at 3 months although these changes did not reach statistical significance (P>0.05). There were no significant differences in the changes in the ECVs between the six myocardial segments.

Changes in serum biomarkers

The levels of HCT, creatine kinase MB (CK-MB), and high-density lipoprotein cholesterol (HDL-C) decreased significantly from baseline to the 3-month follow-up (P<0.01); C-reactive protein (CRP), glucose (GLU), and triglyceride (TG) levels increased significantly (P<0.05); and the levels of N-terminal pro-B-type natriuretic peptide (NT-pro-BNP), high-sensitivity cardiac troponin T (hs-cTnT), myohemoglobin (MYO), cholesterol (CHOL), and low-density lipoprotein cholesterol (LDL-C) did not change significantly (Table S2).

Cancer therapy-related cardiac dysfunction

Cancer therapy-related cardiac dysfunction occurred in two patients at the 3-month follow-up. One patient had a new NT-pro-BNP abnormality, and NT-pro-BNP was significantly elevated in one patient at the 3-month follow-up.

Concurrent association between changes in UCG and CCT parameters and myocardial ECV changes

Changes in the UCG parameters and CCT-LVEF did not correlate with any of the changes in the ECVs between baseline and the 3-month follow-up. The changes in CCT-LVEDV indexed were moderately correlated with the changes in the midanteroseptal ECV (r=0.43; P=0.006), midaverage ECV (r=0.45; P=0.004), and global ECV

Table 3 CCT parameters in the patients at baseline and at 3-month follow-up

Parameter	Baseline	3 months	P value
CCT-LVESV indexed, mL/m^2	24.5±6.0	25.4±6.8	0.37
CCT-LVEDV indexed, mL/m^2	71.3±9.4	71.8±9.6	0.69
CCT-LVSV indexed, mL/m^2	46.8±6.3	46.4±7.2	0.70
CCT-CO indexed, L/(min·m^2)	3.5±0.6	3.8±0.6	0.01
CCT-LVEF, %	65.4±5.9	64.3±7.4	0.28
LVMI, g/m^2	55.2±6.2	55.0±5.5	0.72
HR, bpm	75.2±11.5	81.7±12.3	<0.01
LVEFV indexed, mL/m^2	33.3±6.6	30.6±8.2	0.01
LVLFV indexed, mL/m^2	13.5±3.7	15.8±4.2	<0.01
LVEFV/LVLFV	2.7±1.1	2.1±0.9	<0.01
LVRV indexed, mL/m^2	2.3±4.1	3.0±4.2	0.23
LVRFI	0.1±0.1	0.1±0.1	0.43

Data are presented as mean ± standard deviation. CCT, cardiac computed tomography; LVESV, left ventricular end-systolic volume; LVEDV, left ventricular end-diastolic volume; LVSV, left ventricular stroke volume; CO, cardiac output; LVEF, left ventricular ejection fraction; LVMI, left ventricular mass index; HR, heart rate; bpm, beats per minute; LVEFV, left ventricular early (passive) filling volume; LVLFV, left ventricular late (active) filling volume; LVRV, left ventricular regurgitation volume; LVRFI, left ventricular regurgitation fraction index.

Table 4 ECV from CCT in the patients at baseline and at 3-month follow-up

Parameter	Baseline	3 months	Δ0-3 m	P value
Midinferoseptal ECV, %	25.7±3.2	27.1±3.9	1.4±5.2	0.10
Midanteroseptal ECV, %	26.6±3.6	28.1±4.0	1.4±5.3	0.09
Midanterior ECV, %	24.0±4.5	25.6±3.1	1.6±4.9	0.04
Midanterolateral ECV, %	25.6±3.3	26.9±4.2	1.3±5.1	0.12
Midinferolateral ECV, %	25.5±4.1	27.1±4.3	1.7±5.8	0.08
Midinferior ECV, %	26.2±3.6	27.4±3.9	1.2±4.2	0.08
Midaverage ECV, %	25.6±2.5	27.0±2.9	1.4±3.5	0.01
Global ECV, %	25.4±2.4	27.3±2.7	1.8±2.9	<0.01

Data are presented as mean ± standard deviation. P value: baseline *vs.* 3 months; Δ0–3 m: 3 months – baseline. ECV, extracellular volume fraction; CCT, cardiac computed tomography.

(r=0.52; P<0.001) (*Figure 3A-3C*). Changes in CCT-LVSV indexed were correlated with the changes in the midinferoseptal ECV (r=0.51; P<0.001), midaverage ECV (r=0.49; P=0.001), and global ECV (r=0.56; P<0.001) (*Figure 3D-3F*). Changes in CCT-CO indexed also correlated with the changes in the midinferoseptal ECV (r=0.62; P<0.001), midinferolateral ECV (r=0.41; P=0.008), midaverage ECV (r=0.48; P=0.002), and global ECV (r=0.40; P=0.010) (*Figure 3G-3J*). The changes in LVEFV indexed was correlated with the changes in the global ECV (r=0.41; P=0.009) (*Figure 3K*).

Discussion

Our study used CCT scans to evaluate myocardial tissue changes in a population of 40 patients with early-stage breast cancer who were undergoing chemotherapy. We observed a significant increase in global ECV in the early

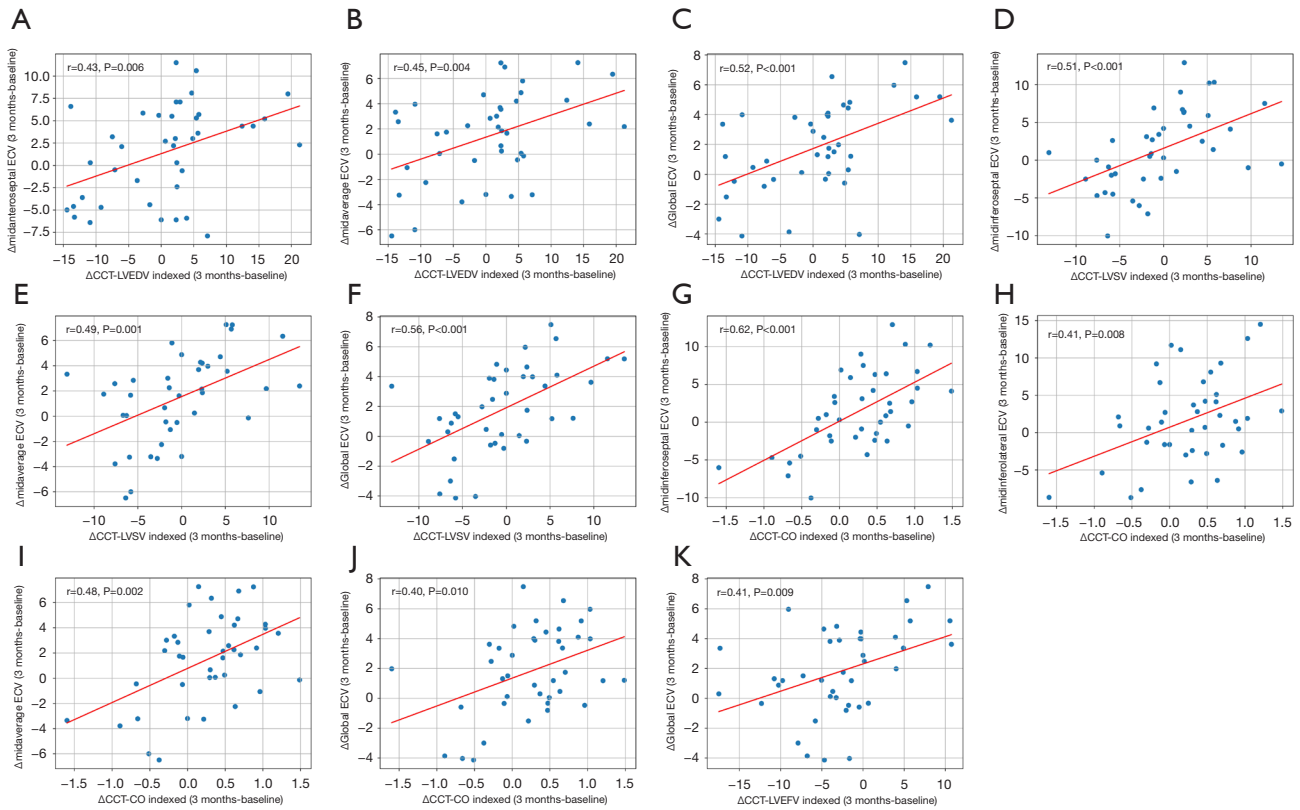

Figure 3 Correlation between changes in cardiac function parameters and ECVs on cardiac computed tomography. Δ, the difference between the third month value and the baseline value (3 months-baseline); ECV, extracellular volume fraction; CCT, cardiac computed tomography; LVEDV indexed, left ventricular end-diastolic volume/body surface area (BSA) ratio; LVSV indexed, left ventricular stroke volume/BSA ratio; CO indexed, cardiac output/BSA ratio; LVEFV indexed, left ventricular early (passive) filling volume/BSA ratio.

stage of chemotherapy, which was correlated with changes in CCT-LVEDV indexed, CCT-LVSV indexed, CCT-CO indexed, and LVEFV indexed. In this study, the ECVs of six myocardial segments had similar degrees of ECV elevation in the early stages of chemotherapy, indicating that the impact of chemotherapy on myocardial tissue is consistent across different regions of the heart.

Although UCG-LVEF is a well-established measure used in clinical practice and has been incorporated within the cancer therapy-related cardiac dysfunction definition, there was no significant decrease in UCG-LVEF or CCT-LVEF during the early stage of chemotherapy in our study. This finding is consistent with a previous study (18) and suggests that myocardial injury in the early stages of treatment may not be sufficiently severe to induce a decline in left ventricular systolic function. There were significant reductions in LVEFV indexed, LVEFV/LVLFV ratio, and e' and an increase in LVLFV indexed at the 3-month follow-up. These parameters reflect changes in cardiac diastolic function earlier than the changes in LVEF in the early stage of chemotherapy. Our findings are consistent with those of Nagiub *et al.*'s (27) study on doxorubicin, where decreases in e' were observed earlier than were the changes in LVEF. Furthermore, abnormal and worsening diastolic dysfunction has been associated with a risk of later systolic dysfunction (28). However, further research is needed to determine whether changes in diastolic function early after chemotherapy are associated with future cancer therapy-related cardiac dysfunction.

In patients with cancer, heart rate has been independently associated with all-cause mortality (29) and reported to be a prognostic factor (30) and significantly increased after anthracycline chemotherapy (31). An increase in heart rate has been independently associated with a subsequent decrease in LVEF (32). Similar to previous studies (31,32), we found in our study that heart rate significantly

increased from 75.2±11.5 to 81.7±12.3 bpm 3 months after anthracycline chemotherapy (P<0.01). The effect of heart rate-lowering therapy in the early antitumor period on lowering the rate of cardiac adverse events is worth exploring.

In our study, the global ECV increased significantly at the 3-month follow-up, earlier than the change in LVEF, which is line with other research (12). Tu *et al.* (18) similarly reported a significant change in ECV 3 months after the initiation of treatment, whereas there were no significant changes in LVEF. Hong *et al.* (33) also found that ECV changed significantly earlier than did the observed changes in LVEF, suggesting that ECV changes are more sensitive and have higher diagnostic value than does LVEF in monitoring early anthracycline-induced cardiotoxicity. ECV might reflect subclinical myocardial injury induced by anthracycline cardiotoxicity before reduced LVEF during early chemotherapy. Our results indicate that ECV can assess early myocardial injury changes with preserved LVEF. Additionally, studies have demonstrated a correlation between ECV and left ventricular diastolic function (34-37). Both myocardial edema and fibrosis, as quantified by ECV, contribute to left ventricular diastolic dysfunction by increasing myocardial stiffness and reducing left ventricular compliance (35). Consequently, changes in ECV are expected to precede the onset of left ventricular diastolic dysfunction, enabling ECV to identify potential cardiotoxicity at an earlier stage. Notably, ECV can still increase despite the administration of dexrazoxane, suggesting that other cardioprotective strategies may be needed. Although changes in ECVs did not correlate with LVEF in our study, they were moderately correlated with partial function parameter. These findings underscore the potential of ECV as an early marker of chemotherapy-induced cardiotoxicity.

UCG is likely to remain the core method for monitoring patients receiving potentially cardiotoxic cancer therapy given its accessibility and extent of information provided. A decrease from baseline in global longitudinal strain (GLS) is used to detect subclinical cardiotoxicity (7). A prospective study reported that declines in GLS can occur in the absence of significant changes in LVEF and can then predict subsequent LV dysfunction (38). GLS monitoring is recommended by the major guidelines despite a lack of trial data supporting a clinically useful benefit, and a number of factors limit the practical utilization of GLS in the real-world oncology setting (39). Therefore, we recommend echocardiographic monitoring including GLS in all patients receiving potentially cardiotoxic cancer therapy (39).

CMR can detect subtle changes that predate clinical symptoms from cancer therapy-related cardiac dysfunction. Anthracyclines first cause an increase in myocardial edema followed by interstitial fibrosis (40); the former can be detected and quantified via T2 mapping, while the latter can be detected via ECV. GLS can also be assessed using CMR (41). However, the limitations of CMR in patients, such as claustrophobia and the risks associated with ferromagnetic devices, need to be considered. Longer imaging times may also be more difficult to endure for some patients. Therefore, CMR may be more suitable for further examination in cases of echocardiography or CCT abnormalities.

In contrast to CMR, CCT provides a more widely available, less expensive, and faster method of ECV quantification and allows for ECV calculation in patients with contraindications to MRI (23). Myocardial ECV quantification with CCT strongly correlates with ECV derived from MRI (23,42). The global ECV in our study (baseline: 25.4%±2.4%; 3 months: 27.3%±2.7%) is nearly consistent with that obtained with CMR reported by Thavendiranathan *et al.* (42) (baseline: 25.3%±2.4%; 53 days: 26.7%±2.7%). It is difficult to convince cancer patients without cardiovascular disease to undergo multiple CMR examinations. If patients are scheduled to undergo chest CT examination regularly before and after treatment, it is easier to add a late enhancement scan (for dual energy acquisitions) to a chest CT scan to acquire ECV as the incremental information (23). This can improve the feasibility and efficiency of the examination and the compliance of the patient. CCT one-stop examination (addition of a late enhancement scan) can simultaneously monitor coronary artery conditions and myocardial ECV changes. A recent study found that coronary artery stenosis and CT fractional flow reserve may serve as imaging markers for predicting cancer therapy-related cardiac dysfunction and recommended the evaluation of coronary parameters in patients (22). Therefore, CCT examination can be regarded as a critical supplement, especially for patients with suspected or preexisting coronary artery disease.

Limitations

Our study involved several limitations which should be discussed. First, the small sample size, mostly a result of the

loss to follow-up (38/56 patients), reduced the statistical power of our analysis. Second, GLS values were not recorded on UCG. Third, as we employed longitudinal observation, the observation time was relatively short. Finally, we included cancer patients with preexisting cardiovascular disease, which reflects the real-world situation of this patient population.

Conclusions

During the early phase after adjuvant chemotherapy, the myocardial ECVs from CCT scans increased significantly before LVEF decreased significantly. The increases in ECV were not correlated with LVEF. The changes in myocardial ECVs were moderately correlated with cardiac function parameters. An early increase in ECV may indicate cardiotoxicity associated with antitumor therapy. It remains to be further determined how certain imaging modalities (UCG, CCT, and CMR) can be integrated into the detection of subclinical cancer therapy-related cardiac dysfunction.

Acknowledgments

We would like to thank nurse Beiyun Xu and Dr. Xiyu Liu for their clinical support and the Philips engineer Ke Chen for his support of the research.

Funding: This work was supported by the Key Project of National Natural Science Foundation of China (No. NSFC82430061), the Special Research Fund for Clinical Studies of Innovative Drugs after Market Launch (No. WKZX2024CX103301), and the Shanghai Pudong Science and Technology Development Fund for Livelihood Scientific Research (No. PKJ2024-Y55).

Footnote

Reporting Checklist: The authors have completed the STROBE reporting checklist. Available at https://qims.amegroups.com/article/view/10.21037/qims-24-777/rc

Conflicts of Interest: All authors have completed the ICMJE uniform disclosure form (available at https://qims.amegroups.com/article/view/10.21037/qims-24-777/coif). W.D. and Y.W. are full-time employees of Clinical & Technical Support Department, Philips Healthcare, during the conduct of the study; and they receive consulting fees from AMCA. The other authors have no conflicts of interest to declare.

Ethics Statement: The authors are accountable for all aspects of the work in ensuring that questions related to the accuracy or integrity of any part of the work are appropriately investigated and resolved. This study was conducted in accordance with the Declaration of Helsinki (as revised in 2013) and was approved by the Ethics Committee of Fudan University Shanghai Cancer Center. Informed consent was obtained from all individual participants (No. 2111245-25; approved on November 30th, 2021).

References

1. Patnaik JL, Byers T, DiGuiseppi C, Dabelea D, Denberg TD. Cardiovascular disease competes with breast cancer as the leading cause of death for older females diagnosed with breast cancer: a retrospective cohort study. Breast Cancer Res 2011;13:R64.
2. Sung H, Ferlay J, Siegel RL, Laversanne M, Soerjomataram I, Jemal A, Bray F. Global Cancer Statistics 2020: GLOBOCAN Estimates of Incidence and Mortality Worldwide for 36 Cancers in 185 Countries. CA Cancer J Clin 2021;71:209-49.
3. Slamon DJ, Leyland-Jones B, Shak S, Fuchs H, Paton V, Bajamonde A, Fleming T, Eiermann W, Wolter J, Pegram M, Baselga J, Norton L. Use of chemotherapy plus a monoclonal antibody against HER2 for metastatic breast cancer that overexpresses HER2. N Engl J Med 2001;344:783-92.
4. McGale P, Darby SC, Hall P, Adolfsson J, Bengtsson NO, Bennet AM, Fornander T, Gigante B, Jensen MB, Peto R, Rahimi K, Taylor CW, Ewertz M. Incidence of heart disease in 35,000 women treated with radiotherapy for breast cancer in Denmark and Sweden. Radiother Oncol 2011;100:167-75.
5. Cardinale D, Colombo A, Bacchiani G, Tedeschi I, Meroni CA, Veglia F, Civelli M, Lamantia G, Colombo N,

Curigliano G, Fiorentini C, Cipolla CM. Early detection of anthracycline cardiotoxicity and improvement with heart failure therapy. Circulation 2015;131:1981-8.
6. Čelutkienė J, Plymen CM, Flachskampf FA, de Boer RA, Grapsa J, Manka R, Anderson L, Garbi M, Barberis V, Filardi PP, Gargiulo P, Zamorano JL, Lainscak M, Seferovic P, Ruschitzka F, Rosano GMC, Nihoyannopoulos P. Innovative imaging methods in heart failure: a shifting paradigm in cardiac assessment. Position statement on behalf of the Heart Failure Association of the European Society of Cardiology. Eur J Heart Fail 2018;20:1615-33.
7. Di Lisi D, Manno G, Novo G. Subclinical Cardiotoxicity: The Emerging Role of Myocardial Work and Other Imaging Techniques. Curr Probl Cardiol 2021;46:100818.
8. Cannaò PM, Altabella L, Petrini M, Alì M, Secchi F, Sardanelli F. Novel cardiac magnetic resonance biomarkers: native T1 and extracellular volume myocardial mapping. Eur Heart J Suppl 2016;18:E64-71.
9. Park HS, Hong YJ, Han K, Kim PK, An E, Lee JY, Park CH, Lee HJ, Hur J, Kim YJ, Choi BW. Ultrahigh-field cardiovascular magnetic resonance T1 and T2 mapping for the assessment of anthracycline-induced cardiotoxicity in rat models: validation against histopathologic changes. J Cardiovasc Magn Reson 2021;23:76.
10. Curigliano G, Lenihan D, Fradley M, Ganatra S, Barac A, Blaes A, et al. Management of cardiac disease in cancer patients throughout oncological treatment: ESMO consensus recommendations. Ann Oncol 2020;31:171-90.
11. Zamorano JL, Lancellotti P, Rodriguez Muñoz D, Aboyans V, Asteggiano R, Galderisi M, Habib G, Lenihan DJ, Lip GYH, Lyon AR, Lopez Fernandez T, Mohty D, Piepoli MF, Tamargo J, Torbicki A, Suter TM; ESC Scientific Document Group. 2016 ESC Position Paper on cancer treatments and cardiovascular toxicity developed under the auspices of the ESC Committee for Practice Guidelines: The Task Force for cancer treatments and cardiovascular toxicity of the European Society of Cardiology (ESC). Eur Heart J 2016;37:2768-801.
12. Hong YJ, Kim TK, Hong D, Park CH, Yoo SJ, Wickum ME, Hur J, Lee HJ, Kim YJ, Suh YJ, Greiser A, Paek MY, Choi BW. Myocardial Characterization Using Dual-Energy CT in Doxorubicin-Induced DCM: Comparison With CMR T1-Mapping and Histology in a Rabbit Model. JACC Cardiovasc Imaging 2016;9:836-45.
13. Bandula S, White SK, Flett AS, Lawrence D, Pugliese F, Ashworth MT, Punwani S, Taylor SA, Moon JC. Measurement of myocardial extracellular volume fraction by using equilibrium contrast-enhanced CT: validation against histologic findings. Radiology 2013;269:396-403.
14. Liang J, Li H, Xie J, Yu H, Chen W, Yin K, Chen X, Sheng Z, Zhang X, Mu D. Iodine-based extracellular volume for evaluating myocardial status in patients undergoing percutaneous coronary intervention for acute myocardial infarction by using dual-layer spectral detector computed tomography: a comparison study with magnetic resonance. Quantitative Imaging in Medicine and Surgery 2022;12:4502-11.
15. Oda S, Nakaura T, Utsunomiya D, Hirakawa K, Takashio S, Izumiya Y, Tsujita K, Hata H, Ando Y, Yamashita Y. Late iodine enhancement and myocardial extracellular volume quantification in cardiac amyloidosis by using dual-energy cardiac computed tomography performed on a dual-layer spectral detector scanner. Amyloid 2018;25:137-8.
16. Monti CB, Zanardo M, Bosetti T, Alì M, De Benedictis E, Luporini A, Secchi F, Sardanelli F. Assessment of myocardial extracellular volume on body computed tomography in breast cancer patients treated with anthracyclines. Quant Imaging Med Surg 2020;10:934-44.
17. Capra D, Monti CB, Luporini AG, Lombardi F, Gumina C, Sironi A, Asti ELG, Bonavina L, Secchi F, Sardanelli F. Computed tomography-derived myocardial extracellular volume: an early biomarker of cardiotoxicity in esophageal cancer patients undergoing radiation therapy. Insights Imaging 2020;11:120.
18. Tu C, Shen H, Liu R, Wang X, Li X, Yuan X, Chen Q, Wang Y, Ran Z, Lan X, Zhang X, Lin M, Zhang J. Myocardial extracellular volume derived from contrast-enhanced chest computed tomography for longitudinal evaluation of cardiotoxicity in patients with breast cancer treated with anthracyclines. Insights Imaging 2022;13:85.
19. Chiocchi M, Cerocchi M, Di Tosto F, Rosenfeld R, Pasqualetto M, Vanni G, De Stasio V, Pugliese L, Di Donna C, Idone G, Muscoli S, Portarena I, Roselli M, Garaci F, Floris R. Quantification of Extracellular Volume in CT in Neoadjuvant Chemotherapy in Breast Cancer: New Frontiers in Assessing the Cardiotoxicity of Anthracyclines and Trastuzumab. J Pers Med 2023;13:199.
20. Egashira K, Sueta D, Tomiguchi M, Kidoh M, Oda S, Usuku H, et al. Cardiac computed tomography-derived extracellular volume fraction in late anthracycline-induced cardiotoxicity. Int J Cardiol Heart Vasc 2021;34:100797.
21. Aquino GJ, O'Doherty J, Schoepf UJ, Ellison B, Byrne J, Fink N, Zsarnoczay E, Wolf EV, Allmendinger T, Schmidt B, Flohr T, Baruah D, Suranyi P, Varga-Szemes A, Emrich T. Myocardial Characterization with Extracellular

Volume Mapping with a First-Generation Photon-counting Detector CT with MRI Reference. Radiology 2023;307:e222030.
22. Tu C, Shen H, Li X, Wang X, Miao Z, Deng W, Liu R, Lan X, Chen H, Zhang J. Longitudinal Evaluation of Coronary Arteries and Myocardium in Breast Cancer Using Coronary Computed Tomographic Angiography. JACC Cardiovasc Imaging 2024;17:1335-47.
23. Cundari G, Galea N, Mergen V, Alkadhi H, Eberhard M. Myocardial extracellular volume quantification with computed tomography-current status and future outlook. Insights Imaging 2023;14:156.
24. Liu P, Lin L, Xu C, Han Y, Lin X, Hou Y, Lu X, Vembar M, Jin Z, Wang Y. Quantitative analysis of late iodine enhancement using dual-layer spectral detector computed tomography: comparison with magnetic resonance imaging. Quant Imaging Med Surg 2022;12:310-20.
25. Mosteller RD. Simplified calculation of body-surface area. N Engl J Med 1987;317:1098.
26. Herrmann J, Lenihan D, Armenian S, Barac A, Blaes A, Cardinale D, et al. Defining cardiovascular toxicities of cancer therapies: an International Cardio-Oncology Society (IC-OS) consensus statement. Eur Heart J 2022;43:280-99.
27. Nagiub M, Nixon JV, Kontos MC. Ability of Nonstrain Diastolic Parameters to Predict Doxorubicin-Induced Cardiomyopathy: A Systematic Review With Meta-Analysis. Cardiol Rev 2018;26:29-34.
28. Upshaw JN, Finkelman B, Hubbard RA, Smith AM, Narayan HK, Arndt L, Domchek S, DeMichele A, Fox K, Shah P, Clark A, Bradbury A, Matro J, Adusumalli S, Carver JR, Ky B. Comprehensive Assessment of Changes in Left Ventricular Diastolic Function With Contemporary Breast Cancer Therapy. JACC Cardiovasc Imaging 2020;13:198-210.
29. Anker MS, Frey MK, Goliasch G, Bartko PE, Prausmüller S, Gisslinger H, Kornek G, Strunk G, Raderer M, Zielinski C, Hülsmann M, Pavo N. Increased resting heart rate and prognosis in treatment-naïve unselected cancer patients: results from a prospective observational study. Eur J Heart Fail 2020;22:1230-8.
30. Lee DH, Park S, Lim SM, Lee MK, Giovannucci EL, Kim JH, Kim SI, Jeon JY. Resting heart rate as a prognostic factor for mortality in patients with breast cancer. Breast Cancer Res Treat 2016;159:375-84.
31. Stoodley PW, Richards DA, Boyd A, Hui R, Harnett PR, Meikle SR, Byth K, Stuart K, Clarke JL, Thomas L. Left ventricular systolic function in HER2/neu negative breast cancer patients treated with anthracycline chemotherapy: a comparative analysis of left ventricular ejection fraction and myocardial strain imaging over 12 months. Eur J Cancer 2013;49:3396-403.
32. Kintsu M, Odajima S, Takeuchi K, Ichikawa Y, Todo S, Ota E, Yamauchi Y, Shiraki H, Yamashita K, Fukuda T, Hisamatsu E, Minami H, Hirata KI, Tanaka H. Effect of increase in heart rate after anthracycline chemotherapy on subsequent left ventricular dysfunction. J Cardiol 2024;84:119-25.
33. Hong YJ, Park HS, Park JK, Han K, Park CH, Kim TK, Yoo SJ, Lee JY, Kim PK, Hur J, Lee HJ, Kim YJ, Suh YJ, Paek MY, Choi BW. Early Detection and Serial Monitoring of Anthracycline-Induced Cardiotoxicity Using T1-mapping Cardiac Magnetic Resonance Imaging: An Animal Study. Sci Rep 2017;7:2663.
34. Neilan TG, Coelho-Filho OR, Shah RV, Feng JH, Pena-Herrera D, Mandry D, Pierre-Mongeon F, Heydari B, Francis SA, Moslehi J, Kwong RY, Jerosch-Herold M. Myocardial extracellular volume by cardiac magnetic resonance imaging in patients treated with anthracycline-based chemotherapy. Am J Cardiol 2013;111:717-22.
35. Maragiannis D, Alvarez PA, Ghosn MG, Chin K, Hinojosa JJ, Buergler JM, Shah DJ, Nagueh SF. Left ventricular function in patients with hypertrophic cardiomyopathy and its relation to myocardial fibrosis and exercise tolerance. Int J Cardiovasc Imaging 2018;34:121-9.
36. Bojer AS, Sørensen MH, Madsen SH, Broadbent DA, Plein S, Gæde P, Madsen PL. The independent association of myocardial extracellular volume and myocardial blood flow with cardiac diastolic function in patients with type 2 diabetes: a prospective cross-sectional cohort study. Cardiovasc Diabetol 2023;22:78.
37. Miura H, Koseki M, Ide S, Asaumi Y, Morita Y, Ohta Y, Tanaka K, Okada T, Omatsu T, Ogata S, Fukuda T, Sakata Y, Noguchi T. Stronger positive correlation of the left ventricular mass index and extracellular volume fraction with diastolic function in diabetic patients without myocardial infarction. Int J Cardiol 2024;408:132099.
38. Negishi K, Negishi T, Hare JL, Haluska BA, Plana JC, Marwick TH. Independent and incremental value of deformation indices for prediction of trastuzumab-induced cardiotoxicity. J Am Soc Echocardiogr 2013;26:493-8.
39. Ruane L, Prasad S, Atherton J. Straining for More Evidence. JACC CardioOncol 2023;5:711-4.
40. Farhad H, Staziaki PV, Addison D, Coelho-Filho OR, Shah RV, Mitchell RN, Szilveszter B, Abbasi SA, Kwong RY, Scherrer-Crosbie M, Hoffmann U, Jerosch-Herold

M, Neilan TG. Characterization of the Changes in Cardiac Structure and Function in Mice Treated With Anthracyclines Using Serial Cardiac Magnetic Resonance Imaging. Circ Cardiovasc Imaging 2016;9:e003584.
41. O'Quinn R, Ferrari VA, Daly R, Hundley G, Baldassarre LA, Han Y, Barac A, Arnold A. Cardiac Magnetic Resonance in Cardio-Oncology: Advantages, Importance of Expediency, and Considerations to Navigate Pre-Authorization. JACC CardioOncol 2021;3:191-200.
42. Thavendiranathan P, Shalmon T, Fan CS, Houbois C, Amir E, Thevakumaran Y, Somerset E, Malowany JM, Urzua-Fresno C, Yip P, McIntosh C, Sussman MS, Brezden-Masley C, Yan AT, Koch CA, Spiller N, Abdel-Qadir H, Power C, Hanneman K, Wintersperger BJ. Comprehensive Cardiovascular Magnetic Resonance Tissue Characterization and Cardiotoxicity in Women With Breast Cancer. JAMA Cardiol 2023;8:524-34.

Cite this article as: Wu H, Huang Y, Yang M, Lu Z, Deng W, Wang Y, Xiao Q, Gu Y. Quantitative assessment of early changes in myocardial extracellular volume during postoperative adjuvant chemotherapy in patients with breast cancer via dual-layer spectral detector computed tomography: a cohort study. Quant Imaging Med Surg 2025;15(1):404-416. doi: 10.21037/qims-24-777